Casimir force on real materials—the slab and cavity geometry

2007 J. Phys. A: Math. Theor. 40 3643

(http://iopscience.iop.org/1751-8121/40/13/021)

IOP PUBLISHING JOURNAL OF PHYSICS A: MATHEMATICAL AND THEORETICAL

J. Phys. A: Math. Theor. **40** (2007) 3643–3664 doi:10.1088/1751-8113/40/13/021

Casimir force on real materials—the slab and cavity geometry

Simen A Ellingsen[1] **and Iver Brevik**

Department of Energy and Process Engineering, Norwegian University of Science and Technology, N-7491 Trondheim, Norway

E-mail: iver.h.brevik@ntnu.no

Received 3 November 2006, in final form 12 February 2007
Published 14 March 2007
Online at stacks.iop.org/JPhysA/40/3643

Abstract

We analyse the potential of the geometry of a slab in a planar cavity for the purpose of Casimir force experiments. The force and its dependence on temperature, material properties and finite slab thickness are investigated both analytically and numerically for the slab and walls made of aluminium and teflon FEP respectively. We conclude that such a setup is ideal for measurements of the temperature dependence of the Casimir force. By numerical calculation it is shown that temperature effects are dramatically larger for dielectrics, suggesting that a dielectric such as teflon FEP whose properties vary little within a moderate temperature range, should be considered for experimental purposes. We finally discuss the subtle but fundamental matter of the various Green's two-point function approaches present in the literature and show how they are different formulations describing the same phenomenon.

PACS numbers: 05.30.−d, 12.20.Ds, 32.80.Lg, 41.20.Jb, 42.50.Nn

1. Introduction

The Casimir effect [1] can be seen as an effect of the zero-point energy of vacuum which emerges due to the non-commutativity of quantum operators upon quantization of the electromagnetic (EM) field. Although formally infinite in magnitude, the EM field density in bulk undergoes finite alterations when dielectric or metal boundaries are introduced in the system, giving rise to finite and measurable forces. As is well known, at nanometre to micrometre separations the Casimir attraction between bodies becomes significant, and the effect has attracted much attention during the last decade in the wake of the rapid advances in nanotechnology. The existence of the Casimir force was shown experimentally as early as 1958 by Spaarnay [2], yet only recently new and much more precise measurements of Lamoreaux and others (see the review [3]) have boosted the interest in the effect from a much broader

[1] Present address: Department of War Studies, King's College London, Strand, London WC2R 2LS, UK.

audience. Experiments like that of Mohideen and Roy [4], and the very recent one of Harber *et al* [5], making use of the oscillations of a magnetically trapped Bose–Einstein condensate, were subject to widespread regard. The same was true for the nonlinear micromechanical Casimir oscillator experiment of Chan *et al* [6, 7].

Recent reviews on the Casimir effect are given in [3, 8–11]. Much information about recent developments can also be found in the special issues of *J. Phys. A: Math. Gen.* (May 2006) [12] and of *New J. Phys.* (October 2006) [13].

Actual calculations of Casimir forces are usually performed via two different routes [8]; either by summation of the energy of discrete quantum modes of the EM field (cf, for instance, [14]), or via a Green's function method first developed by Lifshitz [15]. Mode summation, despite its advantage of a simpler and more transparent formalism, is usually far inferior. In practice it is only in systems where quantum energy states are known that energy summation can be carried out explicitly. This requires the system to be highly symmetric, and favour assumptions such as perfectly conducting walls like in the original Casimir problem. Geometries in which quantum states are known exactly, unfortunately, are few.

The method of calculating the force through Green's functions avoids some but not all of these problems; exact solutions are still only known in highly symmetrical systems such as infinitely large parallel plates or concentric spheres. Via the fluctuation–dissipation theorem, the EM field energy density is linked directly to the photonic Green's function, and the force surface density acting on boundaries can be calculated, at least in principle. The theory of Green's functions and the application of them will be central in the present paper.

The purpose of the present work is twofold. First, we intend to explore some of the delicate issues that occur in the Green's function formalism in typical settings involving dielectric boundaries. Upon relating the two-point functions to Green's function one may choose to calculate the Green function in full [8, 16]. The method is complete but may appear cumbersome, at least so in the presence of several dielectric surfaces. It is possible to reduce the calculational burden somewhat by simplifying the Green function expressions, by omitting those parts that do not contribute to the Casimir force. This means that one works with 'effective' Green functions. This method is employed and briefly discussed by Lifshitz and co-workers; cf e.g. [17]. The connections between the different kinds of Green's functions are in our opinion far from trivial, and we therefore believe it of interest to present some of the formulae that we have compiled and which have turned out to be useful in practice.

As for the calculational technique for the Casimir force in a multilayer system, there exists a powerful formalism worked out, in particular, by Tomaš [18]. In turn, this formalism was based on work by Mills and Maradudin two decades earlier [19]. One of us recently made a review of this technique, with various applications [20]. We shall make use of this technique in the following. In company with the by now classic theory of Lifshitz and co-workers [15, 21] and the standard Fresnel theory in optics, the necessary set of tools is provided.

Our second purpose is to apply the formalism to concrete calculations of the Casimir pressure on a dielectric plate in a multilayer setting. Especially, we will consider the pressure on a plate situated in a cavity (five-zone system). We work out force expressions and eigenfrequency changes when the plate is acted upon by a harmonic-oscillator mechanical force (spring constant k) in addition to the Casimir force, and is brought to oscillate horizontally. To our knowledge, explicit calculations of this sort have not been made before. A chief motivation for this kind of calculation is that we wish to evaluate the magnitudes of thermal corrections to the Casimir pressure. In recent years there have been lively discussions in the literature about the thermal corrections; for some statements of both sides of the controversy; see [16, 22–29]. We hope that the consideration of planar multilayer systems may provide additional insight into the temperature problem.

We will be considering uniformly heated systems only. The recent experiment of Harber *et al* [5] investigated the surface-atom force at thermal equilibrium at room temperature, the goal being to measure the surface-atom force at very large distances, taking into account the peculiar properties of a Bose–Einstein condensate gas. Later, the same group investigated the non-equilibrium effect [30]. This paper seems to have reported the first accurate measurement of the thermal effect (of any kind) of the Casimir force, in good agreement with earlier theoretical predictions [31] (cf also the prior theory of Pitaevskii on the non-equilibrium dynamics of EM fluctuations [32]). Consideration of such systems lies, however, outside the scope of the present paper.

The following point ought also to be commented upon, although it is not a chief ingredient of the present paper: Our problem bears a relationship to the famous Abraham–Minkowski controversy, or more generally the question of how one should construct the correct form of the EM energy–momentum tensor in a medium. This problem has been discussed more and less intensely ever since Abraham and Minkowski proposed their energy–momentum expressions around 1910. The advent of accurate experiments, in particular, has aided a better insight into this complicated aspect of field–matter interacting systems. Some years ago, one of the present authors wrote a review of the experimental status in the field [33] (cf also [34]). There is by now a rather extensive literature in this field; some papers are listed in [35–42]. In the present case, where the EM surface force on a dielectric boundary results from integration of the volume force density across the boundary region, the Abraham and Minkowski predictions actually become equal. Recently, in a series of papers Raabe and Welsch have expressed the opinion that the Abraham–Minkowski theory is inadequate and that a different form of the EM energy–momentum tensor has to be employed [43–46]. We cannot agree with this statement, however. All the experiments in optics that we are aware of can be explained in terms of the Abraham–Minkowski theory in a straightforward way. One typical example is provided, for instance, by the oscillations of a water droplet illuminated by a laser pulse. Some years ago, Zhang and Chang made an experiment in which the oscillations of the droplet surface were clearly detectable [47]. It was later shown theoretically how the use of the Abraham–Minkowski theory could reproduce the observed results to a reasonable accuracy [48, 49]. In our theory below, we will use the Abraham–Minkowski theory throughout.

SI units are used throughout the calculations, and permittivity ϵ and permeability μ are defined as relative (nondimensional) quantities. We thus write $\mathbf{D} = \epsilon_0 \epsilon \mathbf{E}$, $\mathbf{B} = \mu_0 \mu \mathbf{H}$.

The outline of the paper is as follows. In the next section we analyse the 5-layered magnetodielectric system (figure 1), presenting the full Green's function as well as its effective (or reduced) counterpart. We here aim at elucidating some points in the formalism that in our opinion are rather delicate. Section 3 is devoted to a study of an oscillating slab in a Casimir cavity, permitting, in principle at least, how the change in the eigenfrequency of the slab with respect to the temperature can give us information about the temperature dependence of the Casimir force. Section 4 discusses more extensively the relationships between the Green's two-point functions as introduced by Lifshitz *et al* and by Schwinger *et al*. In section 5 we present results of numerical Casimir force calculations for selected substances, taking Al as example of a metal, and teflon FEP as example of a dielectric[2]. In section 6 we consider the effect of finite slab thickness, i.e. the 'leakage' of vacuum radiation from one gap to the other.

[2] As a word of caution, we mention here that our permittivity data for metals are intended to hold in the bulk, whereas in practice the real and imaginary parts of the index of refraction for metals come from ellipsometry measurements, and are thus really *surface* measurements. There is an inherent uncertainty in the calculated results coming from this circumstance, of unknown magnitude, although in our opinion the corrections will hardly exceed the 1% level due to the general robustness of the force expression against permittivity variations. Ideally, information about the permittivity versus imaginary frequency would be desirable, for a metallic film. We thank Steve Lamoreaux for comments on this point.

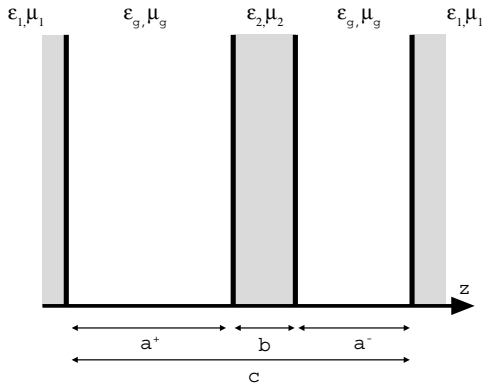

Figure 1. The five-zone geometry of a slab in a cavity. We have chosen $z = 0$ at the left-hand cavity wall.

We find the striking result that for dielectrics the relative finite thickness correction is much larger than for metals. For teflon FEP versus Al the relative correction is almost two orders in magnitude higher.

A word is called for, as regards the permeability μ. As anticipated above, we allow μ to be different from 1. This is motivated chiefly by completeness, and is physically an idealization. It is known that the permeability for most materials is lossy at high frequencies, corresponding to imaginary values for μ. That phenomenon is limited to a restricted frequency interval, however, (10–100 GHz), and loses effect at the higher frequencies.

2. Casimir force on a slab in a cavity

We shall consider a five-layered magnetodielectric system such as depicted in figure 1. The analytical calculation of the Casimir force density acting on the slab in such a geometry is well known; it may be calculated, quite simply, by a straightforward generalization of the famous calculation by Lifshitz and co-workers used for the simpler, three-layered system of two half-spaces separated by a gap [17, 21].

Rather than starting from the photonic Green's function as a propagator as known from quantum electrodynamics, we introduce classical and macroscopic two-point (Green's) function according to the convention of Schwinger *et al* [52] as

$$\boldsymbol{E}(x) = \frac{1}{\epsilon_0}\int \mathrm{d}^4x' \overleftrightarrow{\boldsymbol{\Gamma}}(x,x')\cdot\boldsymbol{P}(x'), \tag{1}$$

where $x = (\boldsymbol{r}, t)$. Due to causality, t' is only integrated over the region $t' \leqslant t$. It follows from Maxwell's equations that Γ obeys the relation

$$\nabla\times\nabla\times\overleftrightarrow{\boldsymbol{\Gamma}}(\boldsymbol{r},\boldsymbol{r}';\omega) - \frac{\epsilon(\boldsymbol{r})\mu(\boldsymbol{r})\omega^2}{c^2}\overleftrightarrow{\boldsymbol{\Gamma}}(\boldsymbol{r},\boldsymbol{r}';\omega) = \frac{\mu(\boldsymbol{r})\omega^2}{c^2}\delta(\boldsymbol{r}-\boldsymbol{r}')\overleftrightarrow{\mathbf{1}}, \tag{2}$$

where we have performed a Fourier transformation according to

$$\overleftrightarrow{\boldsymbol{\Gamma}}(x,x') = \int_{-\infty}^{\infty}\frac{\mathrm{d}\omega}{2\pi}\,\mathrm{e}^{-\mathrm{i}\omega\tau}\overleftrightarrow{\boldsymbol{\Gamma}}(\boldsymbol{r},\boldsymbol{r}';\omega), \tag{3}$$

with $\tau \equiv t - t'$.

A comparison of (2) with the corresponding equation in [17, 21] shows formally that Γ is essentially equivalent with the retarded photonic Green's function in a medium[3]. The physical connection is not entirely trivial, however. As motivation we note that (1) expresses the linear relation between the dipole density at x' and the resulting electric field at x, in essence the extent to which an EM field is able to *propagate* from x' to x. This is exactly the classical analogy of the quantum definition of a Green's function propagator, in accordance with the correspondence principle as introduced by Niels Bohr in 1923. We note furthermore that insisting that $t' \leqslant t$ ensures that account is taken of retardation, corresponding to the Lifshitz definition of the retarded photonic Green's function (e.g. [17, section 75]) which is 0 for $t < t'$.

We make use of the fluctuation–dissipation theorem at zero temperature, rendered conveniently as

$$\mathrm{i}\langle E_i(\boldsymbol{r})E_k(\boldsymbol{r}')\rangle_\omega = \frac{\hbar}{\epsilon_0}\,\Im\mathrm{m}\{\Gamma_{ik}(\boldsymbol{r},\boldsymbol{r}';\omega)\} \tag{4a}$$

$$\mathrm{i}\langle H_i(\boldsymbol{r})H_k(\boldsymbol{r}')\rangle_\omega = \frac{\hbar}{\mu_0}\frac{c^2}{\mu\mu'\omega^2}\,\mathrm{Curl}_{ij}\,\mathrm{Curl}'_{kl}\,\Im\mathrm{m}\{\Gamma_{jl}(\boldsymbol{r},\boldsymbol{r}';\omega)\}, \tag{4b}$$

with the notation $\mathrm{Curl}_{ik} \equiv \epsilon_{ijk}\partial_j$ (ϵ_{ijk} being the Levi-Civita symbol and summation over identical indices is implied), $\mathrm{Curl}'_{ik} \equiv \epsilon_{ijk}\partial'_j$ where ∂'_j is differentiation with respect to component j of $\boldsymbol{r}'$, and $\mu' \equiv \mu(\boldsymbol{r}')$. The brackets denote the mean value with respect to fluctuations. The Casimir pressure acting on some surface is now given by the zz-component of the Abraham–Minkowski stress tensor, found by simple insertion to become [17, 21][4]

$$\mathcal{F}_z = \hbar\int_0^\infty \frac{\mathrm{d}\zeta}{2\pi}\left[\epsilon\left(\Gamma^E_{xx}+\Gamma^E_{yy}-\Gamma^E_{zz}\right)+\frac{1}{\mu}\left(\Gamma^H_{xx}+\Gamma^H_{yy}-\Gamma^H_{zz}\right)\right]_{r=r'}, \tag{5}$$

where a standard frequency rotation $\omega = \mathrm{i}\zeta$ has been performed and the convenient quantities Γ^E and Γ^H have been defined according to

$$\Gamma^E_{ik}(\boldsymbol{r},\boldsymbol{r}';\omega) \equiv \Gamma_{ik}(\boldsymbol{r},\boldsymbol{r}';\omega), \tag{6a}$$

$$\Gamma^H_{ik}(\boldsymbol{r},\boldsymbol{r}';\omega) \equiv \frac{c^2}{\omega^2}\,\mathrm{Curl}_{il}\,\mathrm{Curl}'_{km}\,\Gamma_{lm}(\boldsymbol{r},\boldsymbol{r}';\omega). \tag{6b}$$

In (5) only the homogeneous (geometry dependent) solution of (2) is included; the inhomogeneous solution pertaining to the delta function represents the solution inside a homogeneous medium filling all of space. This term is geometry independent, and cannot contribute to any physically observable quantity. Importantly, however, any such simplification from the full Green's function to its 'effective' counterpart must only be made subsequent to all other calculations.

The system is symmetrical with respect to translation and rotation in the xy-plane and we transform the Green's function once more:

$$\overleftrightarrow{\boldsymbol{\Gamma}}(\boldsymbol{r},\boldsymbol{r}';\omega) = \int \frac{\mathrm{d}^2k_\perp}{(2\pi)^2}\,\mathrm{e}^{\mathrm{i}\boldsymbol{k}_\perp\cdot(\boldsymbol{r}_\perp-\boldsymbol{r}'_\perp)}\overleftrightarrow{\mathbf{g}}(z,z';\boldsymbol{k}_\perp,\omega). \tag{7}$$

Here and henceforth, the subscript $\perp$ refers to a direction in the xy-plane. In the $\boldsymbol{k}_\perp,\omega$ Fourier domain one finds [8, 52] that the component equations (2) combine to (among others) the equations

$$\left(\partial_z^2-\kappa^2\right)g_{xx}(z,z';\boldsymbol{k}_\perp,\omega) = \frac{\kappa^2}{\epsilon\mu}\delta(z-z') \tag{8}$$

[3] Compared to Lifshitz *et al* $\mathcal{D} = -\hbar c^2\Gamma/\omega^2$, which is only a matter of definition.

[4] The expression is generalized compared to the original reference to allow $\mu \neq 1$.

and

$$\left(\partial_z^2 - \kappa^2\right) g_{yy}(z, z'; \boldsymbol{k}_\perp, \omega) = -\frac{\mu\omega^2}{c^2}\delta(z - z'), \tag{9}$$

which readily give us these two components in each homogeneous zone. We have defined the quantity $\kappa \equiv \left(k_\perp^2 - \epsilon\mu\omega^2/c^2\right)^{1/2}$. The final diagonal component is found by means of the relations

$$g_{zz}(z, z'; \boldsymbol{k}_\perp, \omega) = -\frac{\mathrm{i}k_\perp}{\kappa^2}\partial_z g_{xz}(z, z'; \boldsymbol{k}_\perp, \omega) + \frac{1}{\kappa^2}\frac{\mu\omega^2}{c^2}\delta(z - z') \tag{10a}$$

$$g_{zx}(z, z'; \boldsymbol{k}_\perp, \omega) = -\frac{\mathrm{i}k_\perp}{\kappa^2}\partial_z g_{xx}(z, z'; \boldsymbol{k}_\perp, \omega) \tag{10b}$$

$$g_{xz}(z, z'; \boldsymbol{k}_\perp, \omega) = g_{zx}(z', z; -\boldsymbol{k}_\perp, \omega), \tag{10c}$$

of which the first two are components of (2) and the last was shown by Lifshitz (e.g. [17]).

We return to the geometry of figure 1. An important point to emphasize is that unlike certain authors in the past (e.g. [53]) we make no principal difference between the walls of the cavity and the slab; they are both made of real materials with finite permittivity and conductivity at all frequencies as is the case in any real experimental setting. The net force density per unit transverse area acting on the slab is found by first placing the source (i.e. z') in one of the gaps and calculate the resulting Green's function in this gap. This yields the attraction the stack of layers to the left and right of this gap exert upon each other. The procedure is then repeated with respect to the other gap region and the net force on the slab found as the difference between the two.

The solution of (8) may be written down directly, yielding in the case where z' lies in the gap region to the left of the slab

$$g_{xx} = \begin{cases} A\,\mathrm{e}^{\kappa_1 z} & z < 0 \\ C_1\,\mathrm{e}^{\kappa_g z} + C_2\,\mathrm{e}^{-\kappa_g z} + G\,\mathrm{e}^{-\kappa_g|z-z'|} & 0 < z < a^+ \\ E_1\,\mathrm{e}^{\kappa_2 z} + E_2\,\mathrm{e}^{-\kappa_2 z} & a^+ < z < a^+ + b \\ D_1\,\mathrm{e}^{\kappa_g z} + D_2\,\mathrm{e}^{-\kappa_g z} & a^+ + b < z < c \\ B\,\mathrm{e}^{-\kappa_1 z} & z > c \end{cases} \tag{11}$$

with $G = -\kappa_g/(2\epsilon_g\mu_g)$. The 'constants' A to E are z'-dependent. From standard conditions of EM field continuity and (4*a*) and (4*b*) one may show that g_{xx} and $(\epsilon/\kappa^2)\partial_z g_{xx}$ are continuous across interfaces, giving a total of eight equations which are solved with respect to C_1 and C_2 yielding after lengthy but straightforward calculation (for details, cf [54]) the solution in the left hand gap ($0 < z < a^+$, denoted by superscript +)

$$g_{xx}(+) = -\frac{\kappa_g}{2\epsilon_g}\left\{\frac{1}{d_{\mathrm{TM}}^+}\left[2\cosh\kappa_g(z - z') + \frac{\mathrm{e}^{\kappa_g(z+z')}}{\Delta_1^{\mathrm{TM}}} + \Delta_1^{\mathrm{TM}}\,\mathrm{e}^{-\kappa_g(z+z')}\right] + \Delta_1^{\mathrm{TM}}\,\mathrm{e}^{-\kappa_g(z+z')}\right\}.$$

Here and henceforth the inhomogeneous $|z - z'|$-term has been omitted subsequent to other calculation as argued above. Foreknowingly, we have defined the key quantities

$$\frac{1}{d_q^\pm} = \frac{U_q^\mp\,\mathrm{e}^{-2\kappa_g a^\pm}}{V_q^\mp - U_q^\mp\,\mathrm{e}^{-2\kappa_g a^\pm}}, \qquad q = \{\mathrm{TE}, \mathrm{TM}\} \tag{12}$$

where

$$U_q^\pm = \Delta_{1q}\Delta_{2q}\left(1 - \Delta_{1q}\Delta_{2q}\,\mathrm{e}^{-2\kappa_g a^\pm}\right) - \Delta_{1q}\left(\Delta_{2q} - \Delta_{1q}\,\mathrm{e}^{-2\kappa_g a^\pm}\right)\mathrm{e}^{-2\kappa_2 b},$$
$$V_q^\pm = 1 - \Delta_{1q}\Delta_{2q}\,\mathrm{e}^{-2\kappa_g a^\pm} - \Delta_{2q}\left(\Delta_{2q} - \Delta_{1q}\,\mathrm{e}^{-2\kappa_g a^\pm}\right)\mathrm{e}^{-2\kappa_2 b},$$

using the single-interface Fresnel reflection coefficients

$$\Delta_{i,q} = \frac{\kappa_i - \gamma_{i,q}\kappa_g}{\kappa_i + \gamma_{i,q}\kappa_g}, \qquad \gamma_{i,q} = \begin{cases} \mu_i/\mu_g, & q = \text{TE} \\ \epsilon_i/\epsilon_g, & q = \text{TM}, \end{cases} \qquad i = 1, 2. \tag{13}$$

Note already how the quantity $(d^{\pm})^{-1}$ is a generalization of the quantity d^{-1} as it was defined for the three-layer system by Schwinger *et al* [8, 52] (dubbed Δ in the Lifshitz *et al* literature). In the limit $\kappa_2 \to \kappa_g$ we immediately get $\left(d_q^{\pm}\right)^{-1} \to \left(\Delta_{1q}^{-2}\,\mathrm{e}^{2\kappa_g c} - 1\right)^{-1}$, i.e. the three-layer standard result for a cavity of width c with no slab.

Following the above described procedure we get

$$g_{zz}(+) = \frac{k_\perp^2}{2\kappa_g\epsilon_g}\left\{\frac{1}{d_{\text{TM}}^+}\left[2\cosh\kappa_g(z-z') - \frac{\mathrm{e}^{\kappa_g(z+z')}}{\Delta_1^{\text{TM}}} - \Delta_1^{\text{TM}}\,\mathrm{e}^{-\kappa_g(z+z')}\right] + \Delta_1^{\text{TM}}\,\mathrm{e}^{-\kappa_g(z+z')}\right\}.$$

Exactly the same procedure as for g_{xx} is followed to obtain the yy-component. One finds that g_{yy} and $\mu^{-1}\partial_z g_{yy}$ are continuous across boundaries, giving eight new equations solved as above to yield:

$$g_{yy}(+) = \frac{\mu_g}{2\kappa_g}\frac{\omega^2}{c^2}\left\{\frac{1}{d_{\text{TE}}^+}\left[2\cosh\kappa_g(z-z') - \frac{\mathrm{e}^{\kappa_g(z+z')}}{\Delta_1^{\text{TE}}} - \Delta_1^{\text{TE}}\,\mathrm{e}^{-\kappa_g(z+z')}\right] - \Delta_1^{\text{TE}}\,\mathrm{e}^{-\kappa_g(z+z')}\right\}.$$

The results for the right-hand $(-)$ gap is found by transforming the above results according to $a^{\pm} \to a^{\mp}$ and $z \to c - z, z' \to c - z'$.

To obtain the force density on each side of the slab, the solutions are now inserted into (5). One may show [54] that the terms depending on $z + z'$ do not contribute to the force density (this is a subtle point which will be discussed further below). Upon omitting these terms, the right-hand expressions are simply given by swapping + and − indices everywhere and we are left with the *effective* Green's function solution in the $\omega, k_\perp$-domain:

$$g_{xx}(\pm) = -\frac{\kappa_g}{\epsilon_g}\frac{1}{d_{\text{TM}}^{\pm}}\cosh\kappa_g(z-z') \tag{14a}$$

$$g_{yy}(\pm) = \frac{\omega^2\mu_g}{c^2\kappa_g}\frac{1}{d_{\text{TE}}^{\pm}}\cosh\kappa_g(z-z') \tag{14b}$$

$$g_{zz}(\pm) = \frac{k_\perp^2}{\kappa_g\epsilon_g}\frac{1}{d_{\text{TM}}^{\pm}}\cosh\kappa_g(z-z'). \tag{14c}$$

Upon insertion into (5) we find the force on either side of the slab yielding the net Casimir pressure acting on the slab towards the right as

$$\mathcal{F}^0(a^+, a^-; b, c) = \frac{\hbar}{2\pi^2}\int_0^\infty \mathrm{d}\zeta \int_0^\infty \mathrm{d}k_\perp \cdot k_\perp\kappa_g \sum_{q=\text{TE}}^{\text{TM}}\left(\frac{1}{d_q^-} - \frac{1}{d_q^+}\right). \tag{15}$$

Naturally, the force will always point away from the centre position. Superscript 0 here denotes that the expression is taken at zero temperature. The finite temperature expression, as is well known, is found by replacing the frequency integral by a sum over Matsubara frequencies according to the transition

$$\hbar\int_0^\infty \frac{\mathrm{d}\zeta}{2\pi} f(\mathrm{i}\zeta) \to k_B T {\sum_{m=0}^{\infty}}' f(\mathrm{i}\zeta_m), \qquad \mathrm{i}\zeta_m = \mathrm{i}(2\pi k_B T/\hbar)\cdot m$$

yielding

$$\mathcal{F}^T(a^+, a^-; b, c) = \frac{k_B T}{\pi}{\sum_{m=0}^{\infty}}' \int_0^\infty \mathrm{d}k_\perp \cdot k_\perp\kappa_g \sum_{q=\text{TE}}^{\text{TM}}\left(\frac{1}{d_q^-} - \frac{1}{d_q^+}\right). \tag{16}$$

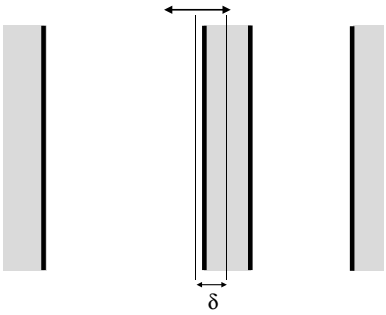

Figure 2. The slab oscillates about the cavity midline. We imagine a spring is attached to the slab exercising a Hooke-force towards the equilibrium position.

The prime on the summation mark denotes that the zeroth term is given half weight as is conventional.

Rather than painstakingly solving the eight continuity equations to obtain the Green's function as above, the result (15) is found much more readily using a powerful procedure following Tomaš as presented recently by one of us [20]. The above result was obtained by Tomaš [55] presumably using this procedure. It was worth going through the above calculations, however, for the sake of shedding light on some in our opinion non-trivial details which are often tacitly bypassed.

3. Casimir measurement by means of an oscillating slab

Equation (16) may be written on a more handy form in terms of the distance δ from the centre of the slab to the midline of the cavity as depicted in figure 2. We introduce the system parameter $h = c - b = a^+ + a^-$ and substitute according to $a^\pm = h/2 \pm \delta$. With some straightforward manipulation we are able to write (16) as

$$\mathcal{F}^T(\delta; b, c) = \frac{k_B T}{\pi} {\sum_{m=0}^{\infty}}' \int_0^\infty \mathrm{d}k_\perp \cdot k_\perp \kappa_g \sum_{q=\mathrm{TE}}^{\mathrm{TM}} \frac{A_q \sinh 2\kappa_g \delta}{B_q - A_q \cosh 2\kappa_g \delta} \tag{17}$$

with

$$A_q = 2\Delta_{1q}\Delta_{2q}(1 - \mathrm{e}^{-2\kappa_2 b})\,\mathrm{e}^{-\kappa_g h},$$
$$B_q = 1 - \Delta_{2q}^2\,\mathrm{e}^{-2\kappa_2 b} + \Delta_{1q}^2\left(\Delta_{2q}^2 - \mathrm{e}^{-2\kappa_2 b}\right)\mathrm{e}^{-2\kappa_g h}.$$

We write the force on the slab at finite temperatures as a Taylor expansion to first order in δ as

$$\mathcal{F}^T(\delta; b, c) = a_1 \delta + \mathcal{O}(\delta^3) \tag{18}$$

with

$$a_1(T; b, c) = \frac{2k_B T}{\pi} {\sum_{m=0}^{\infty}}' \int_0^\infty \mathrm{d}k_\perp \cdot k_\perp \kappa_g^2 \sum_{q=\mathrm{TE}}^{\mathrm{TM}} \frac{A_q}{B_q - A_q}. \tag{19}$$

Assume now the slab is attached to a spring with spring constant k per unit transverse area. For small δ we may assume the slab to oscillate in a harmonic fashion (assuming $k > a_1$ now) with frequency given by Newton's second law as

$$\Omega = \Omega_0 - \Delta\Omega(T) = \sqrt{\frac{k - a_1(T)}{m}},$$

where $\Omega_0 = \sqrt{k/m}$ and m is the mass of the slab per unit transverse area. In the case that $k \gg a_1$ we get

$$\Delta\Omega(T) \approx \frac{a_1(T)}{2\sqrt{km}} = \Omega_0 \frac{a_1(T)}{2k}.$$

We show by numerical calculation in section 5 how the Taylor coefficient $a_1(T)$ varies significantly with T rendering an oscillating slab-in-cavity setup possibly suitable for future experimental investigation of the true temperature dependence of the Casimir force.

The setup as described is somewhat reminiscent of the setup currently employed by Onofrio and co-workers in Grenoble [50] where plates mounted on a double torsion balance are attracted to a pair of fixed plates. In their planned experiment, the distance from plate to wall will however kept constant during force measurements. Indeed, a double torsion balance might be one way of envisioning an experimental realization essentially equivalent to the system described (if thickness corrections are neglected) if the plates are mounted such that when one pair of plates approach each other, separation is increased between the pair on the opposite side of the pendulum. An even closer relative might be the recent experiments in Colorado where perturbations of the eigenfrequency of a magnetically trapped Bose–Einstein substrate in the vicinity of a surface provides a sensitive force measurement technique [5, 30, 51]. Both of these experiments involve a plate (in the widest sense) attracted to a wall on only *one* side; an 'open cavity'.

While a one-sided configuration is possibly experimentally simpler, there are two physical advantages of the sandwich geometry as presented here: the frequency shift $\Delta\Omega(T)$ is essentially twice as large using a closed cavity and, perhaps more importantly, in a symmetrical geometry the harmonical approximation ($\mathcal{F}^T \propto \delta$) is accurate for larger deviations δ from the equilibrium position than is the case for an open geometry. These points are elaborated further in appendix.

4. Fundamental discussion: two-point functions and Green's functions

In the standard Casimir literature there are two famous and somewhat different derivations of the classical Lifshitz expression[5], namely that of Lifshitz and co-workers in 1956–1961 [15, 17] and that of Schwinger and co-workers some years later [8, 52]. The two both make use of a Green's two-point function but in two different ways which upon comparison seem somewhat contradictory at first glance. Understanding how they relate to each other is not trivial in our opinion.

In order to calculate the force acting on an interface between two different media, both schools calculate what in our coordinates is the zz component of the Abraham–Minkowski energy–momentum tensor as described above using the Green's function through the fluctuation–dissipation theorem as in (4*a*) and (4*b*). Lifshitz argues as recited above that in his formalism some terms of the Green's function (those dependent on $z + z'$) make no contribution to the force[6]. These are consequently omitted, leaving an *effective* Green's function. Schwinger *et al*, however, make use of the *entire* Green's function ultimately arriving at an expression similar to (5) in which the $z + z'$ terms *are* included and indeed necessary in order to reproduce Lifshitz' result. The $|z - z'|$-dependent source term is geometry independent and eventually omitted in both references.

[5] By 'Lifshitz force' is henceforth meant the Casimir force between two plane parallel (magneto) dielectric half-spaces separated by a medium different from both. By the 'Lifshitz expression' is meant the mathematical expression for this force as derived by Lifshitz and co-workers [21].

[6] This is shown formally in [54].

To solve the paradox we recognize one important difference between the two procedures: Lifshitz takes the limit $\boldsymbol{r} \to \boldsymbol{r}'$ so that $\boldsymbol{r}$ and $\boldsymbol{r}'$ are both on the same side of one of the sharp interfaces, whereas in Schwinger's method, $\boldsymbol{r}$ is on one side whilst $\boldsymbol{r}'$ is on the other. By using continuity conditions for the EM field, calculations can be carried out with analytic knowledge of the Green's function only on one side of the interface in both cases, thus masking this principal difference. Remembering that T_{zz} is the density of momentum flux in the z-direction, the physical difference between the methods is that whilst Lifshitz calculates the force density as the *net* stream of momentum into one side of the interface, Schwinger *et al*'s expression represents the *entire* stream into one side minus the entire stream out of the other side. Due to conservation of momentum, the procedures are physically equivalent.

The question remains how to interpret the terms dependent on $z + z'$. Arguably, the absolute value of such terms must be arbitrary, since they will depend on the position of an arbitrarily placed origin[7]. Furthermore, since these terms cancel each other perfectly in (5), one may think of them as representing an isotropic flux of photonic momentum, flowing in equal amounts in both directions along the z-axis, giving rise to no measurable effect *inside a homogeneous medium*.

Schwinger, however, insists $\boldsymbol{r}$ and $\boldsymbol{r}'$ lie infinitesimally close to *either side* of an interface. While the $z + z'$ terms cancel each other when all calculated in the same medium, their values depend on ϵ and μ, so when $\epsilon \neq \epsilon'$ or $\mu \neq \mu'$, their net contribution is finite.

This is exactly made up for in Lifshitz' approach by the fact that a sudden change in permittivity and permeability (such as at an interface between a dilute and an opaque medium) causes some of the radiation to be reflected off the interface in accordance with Fresnel's theory. Thus although z and z' both lie inside the same medium, there is a net flow of momentum either out of (attractive) or into (repulsive) the gap giving rise to a Casimir force. Such an analysis of the use of Green's functions gives way for an understanding of how three different representations of the Casimir effect come together; the derivation by Lifshitz starting from photonic propagators in quantum electrodynamics, that by Schwinger *et al* based on Green's function calculations from classical electrodynamics and a third approach based on Fresnel theory which we may refer to as the 'optical approach' (originally in form of non-retarded Van der Waals theory [56, 57], recently revisited by Scardicchio and Jaffe; see [58] and references therein).

We showed that the factors $\left(d_q^{\pm}\right)^{-1}$ were generalized versions of the factors denoted by d^{-1} and $(d')^{-1}$ in Schwinger *et al*'s theory for the three-layer model. These are both special cases of a more general quantity

$$\frac{1}{d_q} = \frac{r_{q\mathrm{L}} r_{q\mathrm{R}}\, \mathrm{e}^{-2\kappa_g a}}{1 - r_{q\mathrm{L}} r_{q\mathrm{R}}\, \mathrm{e}^{-2\kappa_g a}}$$

pertaining to a gap of width a separating planar bodies to the left (L) and right (R) of it whose Fresnel reflection coefficients are $r_{q\mathrm{L}}$ and $r_{q\mathrm{R}}$ respectively. If the media are infinitely large and homogeneous media indexed 1 and 2 respectively, say, $r_{q\mathrm{L}}$ and $r_{q\mathrm{R}}$ are simply $-\Delta_{1q}$ and $-\Delta_{2q}$ from (13); if the bodies are more complex, e.g. has a multilayered structure, their corresponding Fresnel coefficients will be more complicated. This is discussed in detail in [20]. An EM plane wave with momentum $\hbar\mathbf{k}$ is described as $\mathrm{e}^{\mathrm{i}(\mathbf{k}_\perp \cdot \mathbf{r}_\perp + k_z z)}$. In medium g, furthermore, $k_z = \mathrm{i}\kappa_g$ according to Maxwell's equations, i.e. the wave is evanescent in the z-direction if $k_\perp^2 > \epsilon_g \mu_g \omega^2/c^2$ (otherwise propagating). After frequency rotation $\omega^2 \to -\zeta^2$

[7] The notion of arbitrarily large energy densities, of course, is not foreign to Casimir calculations; Casimir's original calculation involved the difference between the apparently infinite energy density of the zero-point photon field in the absence and presence of perfectly conducting interfaces.

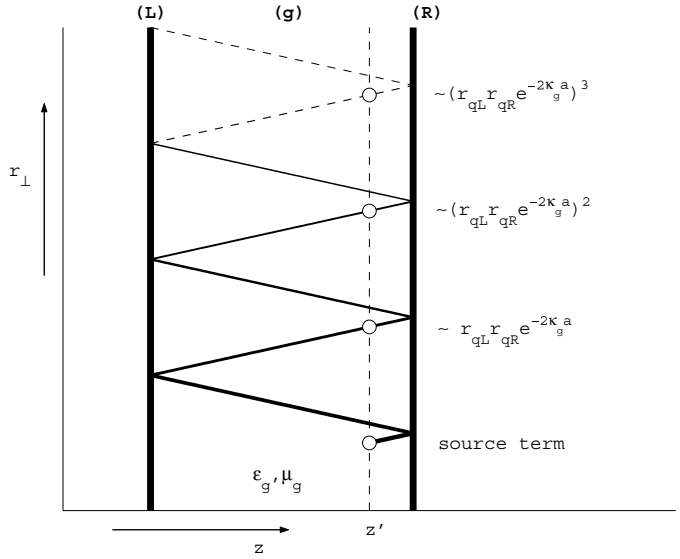

Figure 3. Contributions to $\overleftrightarrow{\mathbf{g}}$ in a gap between two bodies in the optical visualization. The distance between the bodies is a. Each term has a weight factor as shown on the right-hand side. The sum of the infinitely many reflections of a q-polarized wave is d_q^{-1}.

this is always true ($k_\perp$ is assumed real), so *every* wave is described as an evanescent wave. The attenuation of an EM field of frequency $\mathrm{i}\zeta$ propagating a distance l along the z-axis in medium g is $\exp(-\kappa_g l)$, so one readily shows that d_q^{-1} is the sum of *relative amplitudes* of the electric fields having travelled all paths starting and ending at the same z-coordinate and with the same direction:

$$\frac{1}{d_q} = r_{q\mathrm{L}} r_{q\mathrm{R}}\, \mathrm{e}^{-2\kappa_g a} + (r_{q\mathrm{L}} r_{q\mathrm{R}}\, \mathrm{e}^{-2\kappa_g a})^2 + \cdots = \sum_{n=1}^{\infty} (r_{q\mathrm{L}} r_{q\mathrm{R}}\, \mathrm{e}^{-2\kappa_g a})^n .$$

An illustration of this is found in figure 3. Since the phase shift from propagation in the $\perp$ direction is disregarded in this respect, one might think of d_q^{-1} as a sum over all *closed* paths, parallel to the z-axis and starting and ending in the same point.

Considering again the expressions for the complete Green's functions g_{xx}, g_{yy} and g_{zz} in section 2, we see that the last terms of all three components are the only ones not multiplied by a factor d_q^{-1} (indices $\pm$ suppressed). Since this factor is the only part of $\overleftrightarrow{\mathbf{g}}$ containing geometry information, the last term is geometry independent, and can obviously make no contribution to a physical force. Hence, all contributing terms are proportional with d_q^{-1} which leads us to the conclusion that the Casimir attraction between bodies on either side of a gap region at a given temperature depends solely on the extent to which some EM field originating in the gap, stays in the gap.

To sum it all up, we argued that Schwinger's classical Green's function as introduced is the exact macroscopic analogy of Lifshitz' QED propagator according to Bohr's correspondence principle. In its Fourier transformed form it expresses the probability amplitude that an electric field which has transverse momentum $\hbar\mathbf{k}_\perp$, energy $\hbar\omega$ and coordinate z' will give rise to a field of the same energy and momentum at z. When then z and z' are only infinitesimally different, the only way this can happen by classical reasoning is that the two are in fact exactly the same

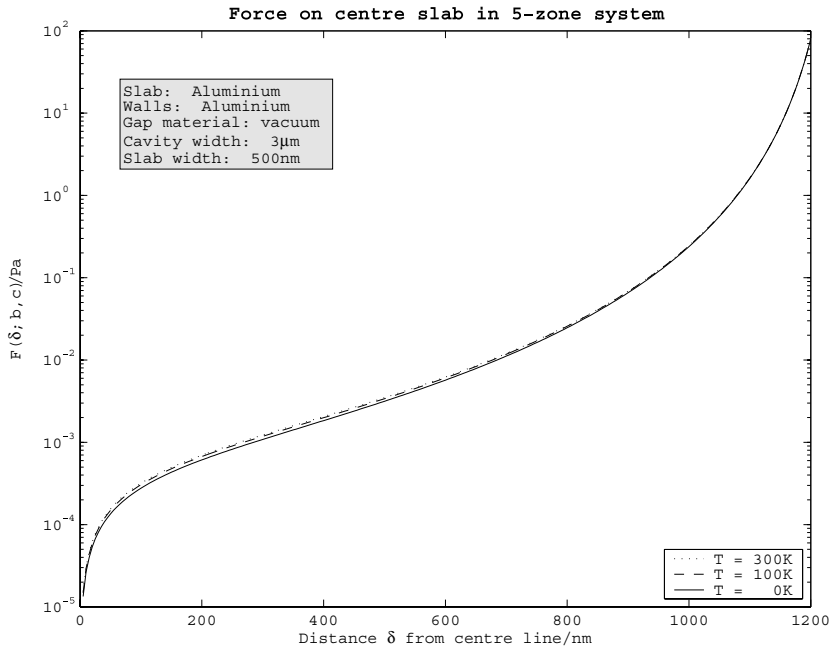

Figure 4. The force on an Al slab in a vacuum-filled cavity between Al walls. δ is the distance from the centre of the slab to the midline of the cavity. For negative δ one gets the antisymmetrical extension of the graph.

(corresponding to the $|z - z'|$-dependent source term) or that the field has been reflected off both walls once or more. This is what figure 3 demonstrates.

5. Numerical investigation and temperature effects

For our numerical calculations, we have used permittivity data for aluminium, gold and copper supplied by Astrid Lambrecht (personal communication). For ease of comparison, aluminium is used in figures throughout; all variations acquired by replacing one metal by another are of a quantitative, not qualitative nature, and are not included here. In all our numerical investigations, we have assumed non-magnetic media, i.e. $\mu_1 = \mu_2 = \mu_g = 1$.

As an example of a dielectric, we have chosen teflon-fluorinated ethylene propylene (teflon FEP) because its chemical and physical properties are remarkably invariant with respect to temperature. Permittivity data for teflon FEP are taken from [59].

Figure 4 shows the Casimir force acting on a relatively thick aluminium slab in a cavity as a function of δ. For negative values of δ the situation is identical but the force has the opposite direction. We have chosen a gap width of 3 μm and a slab thickness of 500 nm. These values are not arbitrary: first, the relative temperature corrections of the Casimir force are predicted to be large at plate separations of 1–3 μm, so a slab-to-wall distance in this region is desirable (here $h/2 = 1250$ nm). Secondly, choosing the slab significantly thicker than the penetration depth of the EM field makes the five-zone geometry instantly comparable to the well-known three-zone Lifshitz geometry of two half-spaces; for slabs of a good metal thicker than $\sim$50 nm there is virtually no difference between the five-zone expression as derived above and that

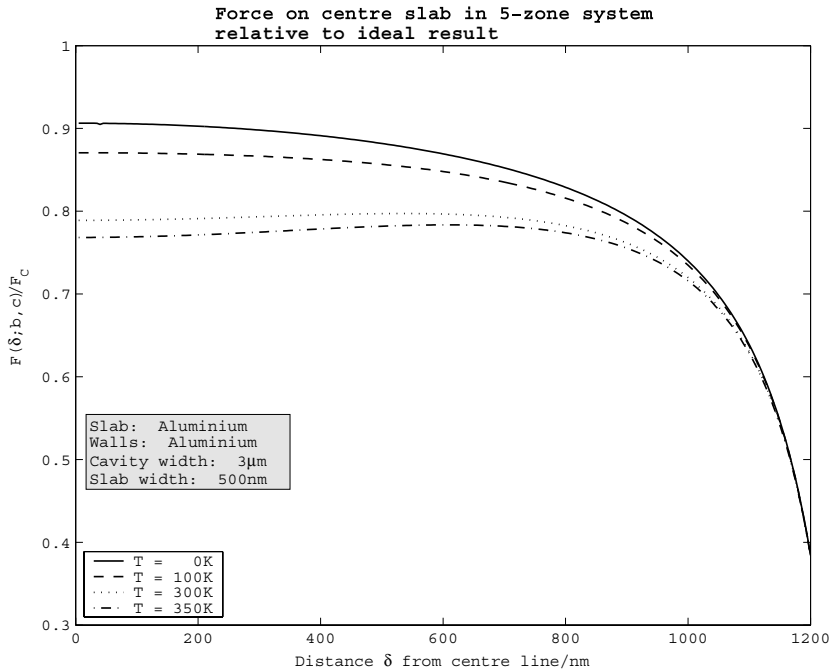

Figure 5. The force on an Al slab in a vacuum-filled cavity between Al walls relative to its value for ideally conducting slab and walls, equation (20). δ is the distance from the centre of the slab to the midline of the cavity. For negative δ one gets the symmetrical extension of the graph.

which one would acquire applying the standard Lifshitz expression to each gap in turn and finding the net force density on the slab as the difference between the two.

Figure 5 shows the net vacuum pressure acting on the slab relative to Casimir's result for ideal conductors,

$$\mathcal{F}_{\mathrm{C}} = \frac{\hbar c \pi^2}{240}\left[\frac{1}{(h/2-\delta)^4} - \frac{1}{(h/2+\delta)^4}\right]. \tag{20}$$

In such a plot we see clearly how a slab and cavity set-up might be suitable for measurements of temperature effects; whereas such effects are small for very small separations, they grow most considerable near the centre position where slab-to-wall distance is in the order of a micrometre.

An altogether different result is obtained upon replacing metal with a dielectric in both walls and slab. In figure 6 the same calculation as in figure 5 has been performed with both slab and walls of teflon FEP. Casimir experiments using dielectrics were proposed by Torgerson and Lamoreaux [60] where the use of diamond was suggested.

It is important to note here that we have not taken into account variations of the dielectric properties of teflon FEP with temperature; much as teflon FEP is renowned for its constancy in electrical and chemical properties over a large temperature range and is used in space technology for this very reason, one must assume there are corrections at extremely low temperatures. We shall not enter into a discussion on material properties here; the point to take on board is rather that temperature effects are found to be very large indeed near the centre position, a fact that does not change should the calculated values be several percent off.

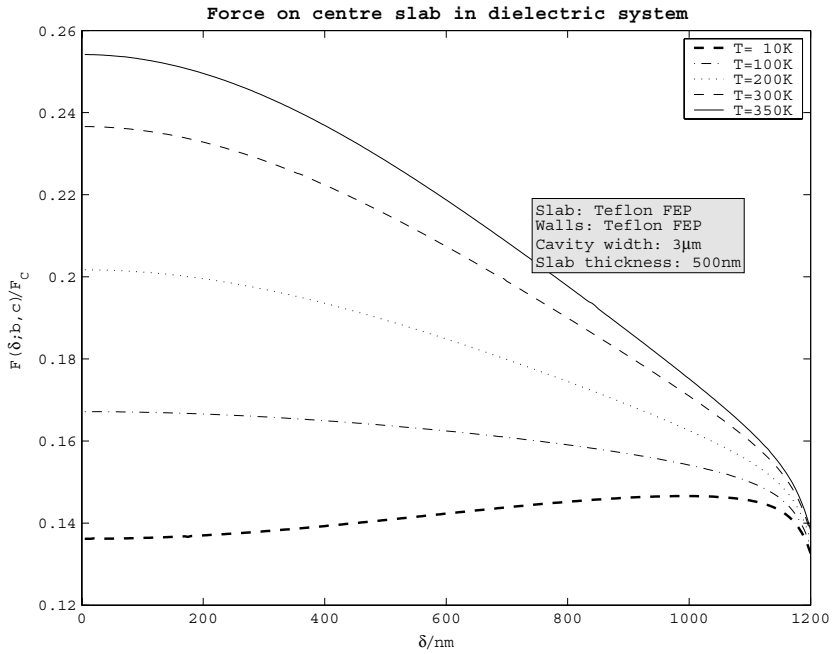

Figure 6. The force on a teflon FEP slab in a vacuum-filled cavity between teflon FEP walls relative to the result for ideally conducting slab and walls, equation (20). Note that dielectric properties are assumed constant with temperature.

This strongly indicates that the use of dielectrics in Casimir experiments could be an excellent means of measuring the still controversial temperature dependence of the force.

We note furthermore that whilst for metals the force decreases with rising temperatures, the opposite is the case for the dielectric. Mathematically this is readily explained from e.g. (16). Temperature enters into the expression in two ways; first, each term of the Matsubara sum has a prefactor T, secondly the distancing of the discrete imaginary frequencies increases linearly with T. The first dependence tends to increase the force with respect to T whilst the other decreases it (bearing in mind that the integrand, which is proportional with $\exp(-\kappa_g h)$, decreases rapidly with respect to ζ for ζ larger than roughly the $m = 1$ Matsubara frequency at room temperature). As temperature rises, thus, the higher order terms of the sum quickly become negligible, leaving the first few terms to dominate[8]. In the high temperature limit, $m = 0$ becomes the sole significant term and the force becomes proportional[9] to T. This is true for metals and dielectrics alike, but while the trend is seen at low temperatures for dielectrics, for metals the T-linear trend typically becomes visible only at temperatures much higher than room temperature. In metals the low (nonzero) frequency terms are boosted since $\epsilon_i \gg \epsilon_g$ for ζ much smaller than the plasma frequency, in which case reflection coefficients $|\Delta_{iq}|$ approximately equal unity. The first few Matsubara terms thus remain significant as temperature rises, countering the T-proportionality effect, at the same time as each $m > 0$ term decreases in value as the Matsubara frequencies take higher values, allowing the resulting force to decrease with increasing temperature.

[8] The same phenomenon for increasing distances rather than temperatures is treated in [62].

[9] For the three-layer Lifshitz set-up, the zero term and thus the force becomes proportional to T/a^3 where a is the gap width, as shown formally in [11].

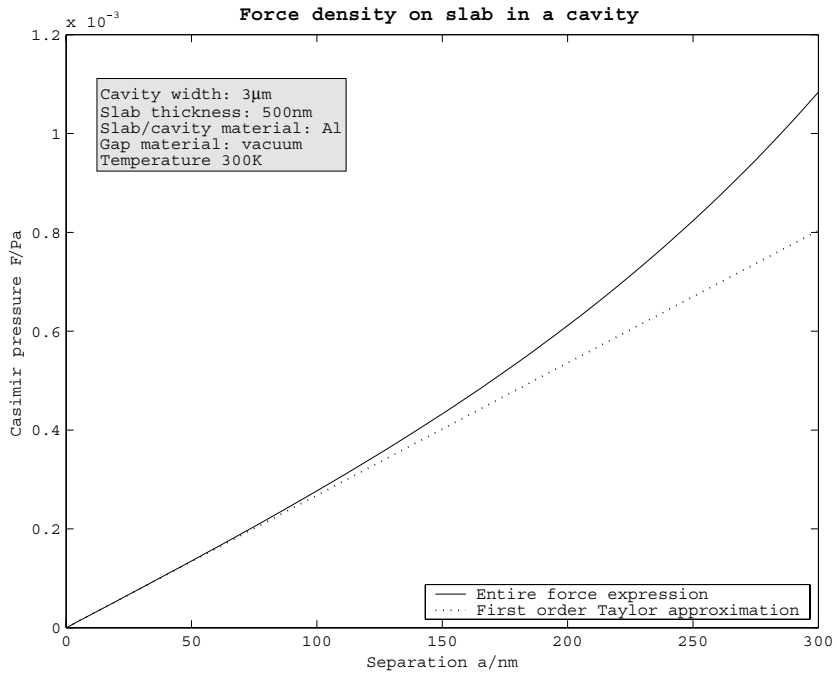

Figure 7. The Casimir force density on the slab of figure 1 as a function of the distance δ from the centre of the slab to the cavity midline as compared to its first-order Taylor expansion, equation (18) at temperature 300 K.

Figure 7 shows the force acting on the slab in the previously described geometry (such as plotted in figure 4) as well the first-order Taylor expansion. The figure gives a rough idea as to the size of the central cavity region in which one may regard the force density as linear with respect to δ. With the system parameters as chosen we see that, depending on precision one may allow oscillation amplitudes δ of several tens of nanometres, a length which is not small relative to the system.

The first-order Taylor coefficient itself has been calculated and plotted in figure 8 for aluminium and teflon FEP slabs in an aluminium cavity. These are furthermore compared to Casimir's ideal result (20) whose first-order Taylor coefficient is readily found to be

$$a_{1\mathrm{C}} = \frac{16\hbar c\pi^2}{15} h^{-5} \approx 3.3283 \times 10^{-25}\ \mathrm{N\,m^2}\ h^{-5}. \tag{21}$$

6. The effect of finite slab thickness

As measurements of the Casimir force have become drastically more accurate over the last few years, with researchers claiming to reproduce theoretical results to within 1% [3, 22], it is well worth asking whether any *theoretical* calculation may rightly claim such an accuracy. A point of particular interest in this respect is the strong dependence of the Casimir force on the permittivity of the media involved. The permittivity data for aluminium, copper and gold supplied by Lambrecht and Reynaud were calculated by using experimental values for the susceptibility at a wide range of real frequencies (approx. 1.5×10^{14} rad s^{-1} $< \omega <$ 1.5×10^{19} rad s^{-1}), extrapolating towards zero frequency by means of the Drude relation (for small

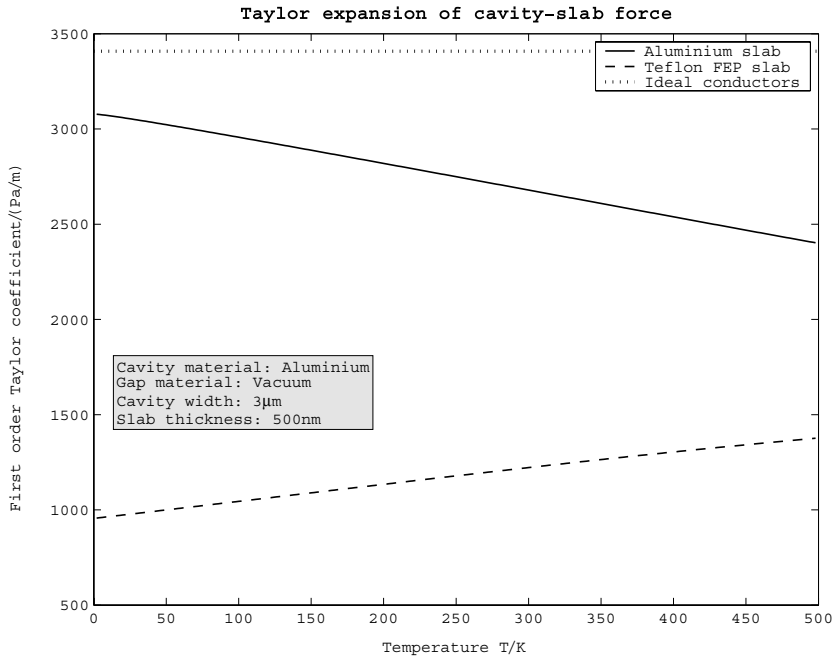

Figure 8. The first-order Taylor coefficient of equation (18) for aluminium and teflon FEP slabs in an Al cavity. The horizontal dotted line is the coefficient pertaining to the Casimir result for ideal conductors (both slab and walls), equation (21). One should note that the dielectric properties of the materials at extremely low temperatures are not known.

$\omega <$ approx 1.5×10^{14} rad s^{-1}). $\epsilon(\omega)$ was subsequently mapped onto the imaginary frequency axis invoking Kramers–Kronig relations numerically. Thus, although matching theoretical values (Drude mode l) excellently for imaginary frequencies up to about 10^{15} rad s^{-1} [24], the data have intrinsic uncertainties. Recently, Lambrecht and co-workers addressed the question of the uncertainty related to calculation of the Casimir force due to uncertainty in the Drude parameters used for extrapolation, found to add up to as much as 5%, considerably more than the accuracy claimed for the best experiments to date [61].

The effect of the 'leakage' of vacuum radiation from one gap region to the other in our five-zone geometry is worth a brief investigation in this context. Excepting the zero frequency term, it is unambiguous from e.g. the definition of κ that when the slab is metallic, the factor $\exp(-2\kappa_2 b)$ is small compared to unity for sufficiently large values of b, due to the large values of ϵ_2 for all important frequencies $\mathrm{i}\zeta$[10]. Let us regard one of the gap regions, of index $\pm$. With some manipulation one may expand (12) to first order in the factor $\exp(-2\kappa_2 b)$ to find the pertaining quantity

$$\frac{1}{d_q^{\pm}} = \frac{\Delta_{1q}\Delta_{2q}\,\mathrm{e}^{-2\kappa_g a^{\pm}}}{1-\Delta_{1q}\Delta_{2q}\,\mathrm{e}^{-2\kappa_g a^{\pm}}} - \mathrm{e}^{-2\kappa_2 b}\frac{\Delta_{1q}\left(1-\Delta_{2q}^2\right)\mathrm{e}^{-2\kappa_g a^{\pm}}}{\left(1-\Delta_{1q}\Delta_{2q}\,\mathrm{e}^{-2\kappa_g a^{\pm}}\right)^2} \cdot \frac{\Delta_{2q}-\Delta_{1q}\,\mathrm{e}^{-2\kappa_g a^{\mp}}}{1-\Delta_{1q}\Delta_{2q}\,\mathrm{e}^{-2\kappa_g a^{\mp}}} + \mathcal{O}(\mathrm{e}^{-4\kappa_2 b}). \tag{22}$$

[10] The $m = 0$ term is a subtle matter we shall not enter into here. For a recent review, see e.g. [29] and references therein.

The first term is immediately recognized as giving the Lifshitz expression for the Casimir attraction between two half-spaces of materials 1 and 2 separated by a gap of width $a^{\pm}$ and material g, and the second term is the first-order correction due to penetration of radiation through the slab.

In terms of δ we may write in the case where $\exp(-2\kappa_2 b) \ll 1$ for all relevant frequencies (again subsequent to some manipulation) the force on the slab as $\mathcal{F}^T(\delta) \approx \mathcal{F}^T_{\rm L} + \Delta\mathcal{F}^T$ where

$$\mathcal{F}^T_{\rm L}(\delta; h) = \frac{k_B T}{\pi} {\sum_{m=0}^{\infty}}' \int_0^{\infty} {\rm d}k_\perp k_\perp \kappa_g \sum_{q={\rm TE}}^{\rm TM} \frac{A_{q{\rm L}} \sinh 2\kappa_g \delta}{B_{q{\rm L}} - A_{q{\rm L}} \cosh 2\kappa_g \delta}$$

is the result using the Lifshitz expression on both gaps and taking the difference; here

$$A_{q{\rm L}} \equiv 2\Delta_{1q}\Delta_{2q}\, {\rm e}^{-\kappa_g h} \qquad \text{and} \qquad B_{q{\rm L}} \equiv 1 + \Delta_{1q}^2 \Delta_{2q}^2\, {\rm e}^{-2\kappa_g h}, \tag{23}$$

and

$$\Delta\mathcal{F}^T(\delta; h, b) = -\frac{k_B T}{\pi} {\sum_{m=0}^{\infty}}' \int_0^{\infty} {\rm d}k_\perp k_\perp \kappa_g \sum_{q={\rm TE}}^{\rm TM} {\rm e}^{-2\kappa_2 b} \times \frac{A_{q{\rm L}}\big(B_{q{\rm L}} - \Delta_{2q}^2 - \Delta_{1q}^2\, {\rm e}^{-2\kappa_g h}\big) \sinh 2\kappa_g \delta}{(B_{q{\rm L}} - A_{q{\rm L}} \cosh 2\kappa_g \delta)^2}. \tag{24}$$

The factor $\exp(-2\kappa_2 b)$ and consequently the first-order correction is very sensitive with respect to even small changes in $\epsilon_2({\rm i}\zeta)$. For very thin slabs ($b < 50$ nm) and small cavities, the correction could be in the order of magnitude of the currently claimed measurement accuracy. Furthermore, we see that the integrand of (24) depends on ϵ_2 in an exponential way. In conclusion: to the extent that the thickness correction is of significance in an experimental measurement, exact knowledge of the permittivity as a function of imaginary frequency is of the essence. In such a scenario, approximate knowledge of the dispersion function could effectively limit our ability to even *calculate* the force with the precision that recent experiments claim to reproduce theory [22]. A calculation of the thickness correction for aluminium slab and walls is shown in figure 9.

In the case of dielectrics, as shown in figure 10, the correction is almost two orders of magnitude larger and should be readily measurable. Experiments in a geometry involving dielectric plates of finite thickness might even be a possible means of evaluating the correctness of the dielectric function employed.

7. Conclusion and final remarks

The main conclusion from the work presented is that from a theoretical point of view the five-zone setup (figure 1) as discussed could be ideal for detection of the temperature dependence of the Casimir force when the wall-to-slab distance is in the order of 1 μm. One method as suggested is a measurement of the difference in the eigenfrequency of an oscillating slab in the absence and presence of a cavity.

When metal is replaced by a dielectric in slab and walls, relative temperature corrections become much larger, suggesting that using dielectrics whose dielectric properties vary little with respect to temperature be excellent for such measurements.

Our treatment of the effect of finite slab thickness shows that the effect of finite thickness varies dramatically with respect to the properties of the materials involved, specifically ϵ and μ. Much as the effect is generally quite small for metals, to the extent such effects do play a role

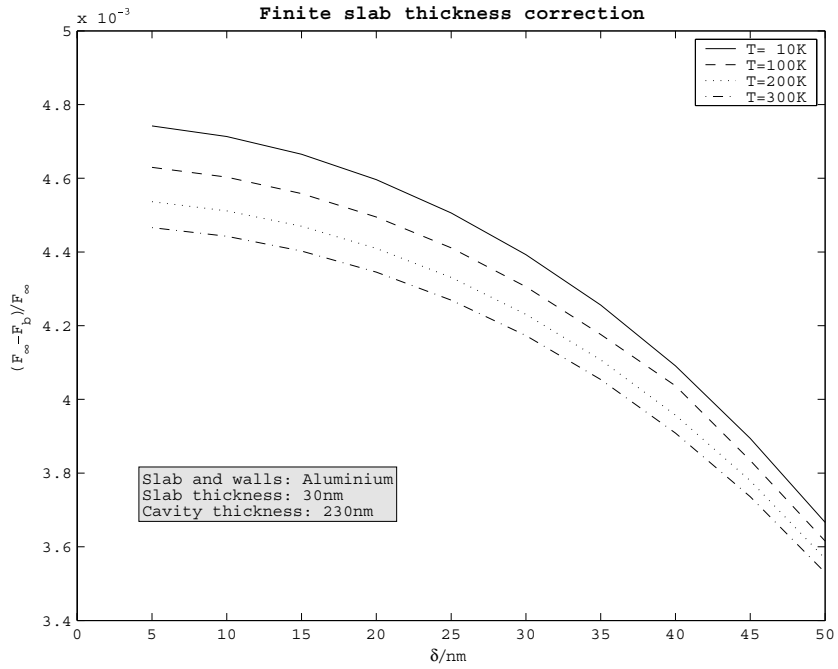

Figure 9. Thickness correction due to 'leakage' of radiation through a thin slab in a small cavity. The absolute value of the correction is approximately exponentially decreasing with the thickness b.

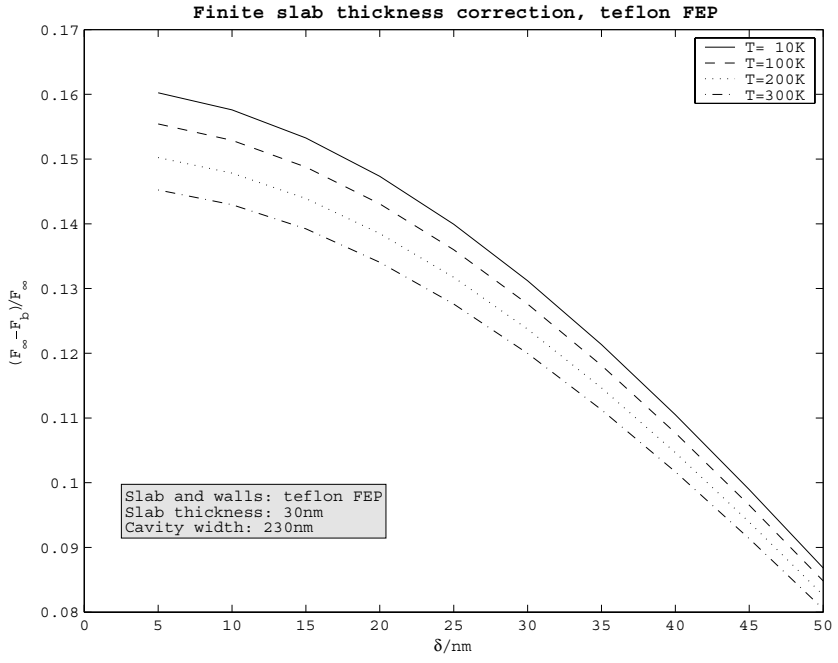

Figure 10. Thickness correction due for teflon FEP.

even a moderately good estimate of their exact magnitude requires very accurate dielectricity data for the material in question. This is but one example of the more general point that the still considerable uncertainties associated with the best available permittivity data for real materials call for soberness in any assessment of our ability to numerically calculate Casimir forces with great precision.

Finally, a couple of remarks: it ought to be pointed out that our proposed method of investigating the thermal Casimir force via observing the oscillations of a slab in a cavity, can be classified as belonging to the subfield usually called the 'dynamic Casimir effect'. The use of mechanical microlevers has turned out to be very effective components for high sensitivity position measurements, of interest even in the context of gravitational waves detection. As for the basic principles of the method see, for instance Jaekel *et al* [63] with further references therein, especially [64]. For more recent papers on microlevers, see [65–68].

Moreover, we note the connection between our approach and the statistical mechanical approach of Buenzli and Martin [69]. These authors computed the force between two quantum plasma slabs within the framework of non-relativistic quantum electrodynamics including quantum and thermal fluctuations of both matter and field. It was found that the difference in the predictions for the temperature dependence of the Casimir effect is satisfactorily explained by taking into account the fluctuations *inside* the material. Their predictions for the force are in agreement with ours.

Acknowledgments

Permittivity data for aluminium, gold and copper used in our calculations were kindly made available to us by Astrid Lambrecht and Serge Reynaud. We furthermore thank Valery Marachevsky for stimulating discussions and input, and Mauro Antezza for valuable correspondence.

Appendix. Closed geometry versus open configuration

We will demonstrate briefly the two physical properties favouring a closed cavity configuration (figure 1) as compared to an open configuration in which a similarly oscillating plate is held in equilibrium by an external spring system. For the purpose of comparison we will disregard effects due to finite plate thickness, so that the net force experienced by a slab in a cavity is the difference between standard Lifshitz forces on both sides, whist that between plate and wall in a one-sided geometry (like figure 1 but with the right-hand wall removed) is simply the Lifshitz force. For separations of some hundred nanometres or more, the Lifshitz force varies as $\mathcal{F}_{\rm L}(d) \propto d^{-4}$. Thus the net force on the slab in the sandwich geometry attached to a spring of spring constant k per unit transverse area is (we assume $k > \mathcal{F}(a)/\delta$ as before)

$$\begin{aligned}\mathcal{F}_{\rm sandwich} &= \mathcal{F}_{\rm L}(a+\delta) - \mathcal{F}_{\rm L}(a-\delta) - k\delta \\ &= \frac{\mathcal{F}_{\rm L}(a)}{(1+\delta/a)^4} - \frac{\mathcal{F}_{\rm L}(a)}{(1-\delta/a)^4} - k\delta \\ &= -\left[ka - 8\,|\mathcal{F}_{\rm L}(a)|\right]\frac{\delta}{a} + 40\,|\mathcal{F}_{\rm L}(a)|\,\frac{\delta^3}{a^3} + \cdots \end{aligned} \tag{A.1}$$

where $a = h/2$ is here the distance from slab to wall in equilibrium position ($\mathcal{F}_{\rm L}(d) < 0$).

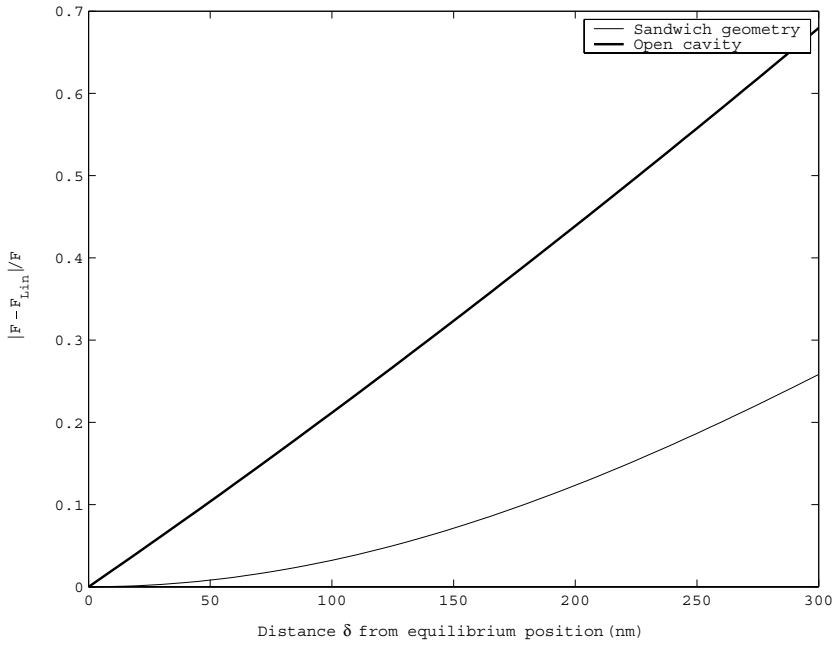

Figure A1. The relative correction to the linear Taylor expansion, $\mathcal{F}_{\rm Lin}$, of the Casimir force near equilibrium position for the open and closed geometries plotted for positive δ. Calculations assume aluminium plate and walls, equilibrium plate-to-wall separation of $a = 1250$ nm in both configurations and temperature 300 K. For the sandwich geometry, $\mathcal{F}$ is given by (16) whilst in the open geometry $\mathcal{F} = \mathcal{F}_{\rm L}(a+\delta) - \mathcal{F}_{\rm L}(a)$ with $\mathcal{F}_{\rm L}$ the standard Lifshitz expression for the attraction between two half-spaces.

Now consider an open configuration in which a plate is held in equilibrium by an external spring, also of spring constant k per unit transverse area. Assume that the forces are in equilibrium when the plate is a distance a from the cavity wall. The net force on the plate is

$$\begin{aligned}\mathcal{F}_{\rm open} &= \mathcal{F}_{\rm L}(a+\delta) - \mathcal{F}_{\rm L}(a) - k\delta \\ &= -[ka - 4|\mathcal{F}_{\rm L}(a)|]\frac{\delta}{a} - 10|\mathcal{F}_{\rm L}(a)|\frac{\delta^2}{a^2} + \cdots . \end{aligned} \tag{A.2}$$

There are thus two properties that favour the closed geometry. First, the first-order perturbation of the spring constant is twice as large and second, that the leading-order correction to the harmonical approximation ($\mathcal{F}^T \propto \delta/a$) is cubical whist it is quadratic for the open configuration[11]. The closed geometry thus allows considerably larger deviations from equilibrium position at a given accuracy without taking non-harmonic effects into account. In figure A1 this is demonstrated by plotting the relative nonharmonic correction as a function of δ at a separation 1250 nm. In accordance with our results, the relative correction $(\mathcal{F} - \mathcal{F}_{\rm Lin})/\mathcal{F}$ is approximately linear for an open geometry $\left(\approx -\frac{5}{2}\frac{\delta}{a}\right)$ and approximately quadratic for a sandwich $\left(\approx 5\frac{\delta^2}{a^2}\right)$.

[11] Note that the specific assumption $\mathcal{F}_{\rm L}(d) \propto d^{-4}$ is not necessary for either of these results; they pertain almost exclusively to geometry. A more general power $\mathcal{F}_{\rm L}(d) \propto d^{-\sigma}$, $\sigma > 0$, say, gives the same properties.

References

[1] Casimir H B G 1948 *Proc. K. Ned. Akad. Wet.* **51** 793
[2] Spaarnay M J 1958 *Physica* **24** 751
[3] Lamoreaux S K 2005 *Rep. Prog. Phys.* **68** 201
[4] Mohideen U and Roy A 1998 *Phys. Rev. Lett.* **81** 4549
[5] Harber D M, Obrecht J M, McGuirk J M and Cornell E A 2005 *Phys. Rev.* A **72** 033610
[6] Chan H B, Aksyuk V A, Kleinman R N, Bishop D J and Capasso F 2001 *Phys. Rev. Lett.* **87** 211801
[7] Chan H B, Aksyuk V A, Kleinman R N, Bishop D J and Capasso F 2001 *Science* **291** 1941
[8] Milton K A 2001 *The Casimir Effect: Physical Manifestation of Zero-Point Energy* (Singapore: World Scientific)
[9] Bordag M, Mohideen U and Mostepanenko V M 2001 *Phys. Rep.* **353** 1
[10] Milton K A 2004 *J. Phys. A: Math. Gen.* **37** R209
[11] Nesterenko V V, Lambiase G and Scarpetta G 2004 *Riv. Nuovo Cimento* **27** (6) 1
[12] 2006 *J. Phys. A: Math. Gen.* **39** (21) (Special issue: Papers Presented at the *7th Workshop on Quantum Field Theory under the Influence of External Conditions (QFEXT05) (Barcelona, Spain, 5–9 Sept. 2005)*
[13] 2006 *New J. Phys.* **8** (234) (Focus issue on Casimir Forces)
[14] Plunien G, Müller B and Greiner W 1986 *Phys. Rep.* **134** 87
[15] Lifshitz E M 1956 *Zh. Eksp. Teor. Fiz.* **29** 94
Lifshitz E M 1956 *Sov. Phys.—JETP* **2** 73 (Engl. Transl.)
[16] Høye J S, Brevik I, Aarseth J B and Milton K A 2003 *Phys. Rev.* E **67** 056116
[17] Lifshitz E M and Pitaevskii L P 1980 *Statistical Physics* Part 2 (Oxford: Pergamon)
[18] Tomaš M S 1995 *Phys. Rev.* A **51** 2545
[19] Mills D L and Maradudin A A 1975 *Phys. Rev.* B **12** 2943
[20] Ellingsen S A 2007 *J. Phys. A: Math. Theor.* **40** 1951 (*Preprint* quant-ph/0607157)
[21] Dzyaloshinskii I E, Lifshitz E M and Pitaevskii L P 1961 *Usp. Fiz. Nauk.* **73** 381
Dzyaloshinskii I E, Lifshitz E M and Pitaevskii L P 1961 *Sov. Phys. Usp.* **4** 153 (Engl. Transl.)
[22] Decca R S, López D, Fischbach E, Klimchitskaya G L, Krause D E and Mostepanenko V M 2005 *Ann. Phys. NY* **318** 37
[23] Brevik I, Aarseth J B, Høye J S and Milton K A 2005 *Phys. Rev.* E **71** 056101
[24] Bentsen V S, Herikstad R, Skriudalen S, Brevik I and Høye J S 2005 *J. Phys. A: Math. Gen.* **38** 9575
[25] Bezerra V B, Decca R S, Fischbach E, Geyer B, Klimchitskaya G L, Krause D E, López D, Mostepananko M and Romero C 2006 *Phys. Rev.* E **73** 028101
[26] Høye J S, Brevik I, Aarseth J B and Milton K A 2006 *J. Phys. A: Math. Gen.* **39** 6031
[27] Mostepanenko V M, Bezerra V B, Decca R, Geyer B, Fischbach E, Klimchitskaya G L, Krause D E, López D and Romero C 2006 *J. Phys. A: Math. Gen.* **39** 6589
[28] Brevik I and Aarseth J B 2006 *J. Phys. A: Math. Gen.* **39** 6187
[29] Brevik I, Ellingsen S A and Milton K A 2006 *New J. Phys.* **8** 236
[30] Obrecht J M, Wild R J, Antezza M, Pitaevskii L P, Stringari S and Cornell E A 2007 *Phys. Rev. Lett.* **98** 063201
[31] Antezza M, Pitaevskii L P and Stringari S 2005 *Phys. Rev. Lett.* **95** 113202
[32] Pitaevskii L P 2000 *Comments At. Mol. Phys.* **1** 363
[33] Brevik I 1979 *Phys. Rep.* **52** 133
[34] Brevik I 1986 *Phys. Rev.* B **33** 1058
[35] Møller C 1972 *The Theory of Relativity* 2nd edn (Oxford: Clarendon) section 7.7
[36] Kentwell G W and Jones D A 1987 *Phys. Rep.* **145** 319
[37] Antoci S and Mihich L 1998 *Eur. Phys. J.* **3** 205
[38] Obukhov Y N and Hehl F W 2003 *Phys. Lett.* A **311** 277
[39] Loudon R, Allen L and Nelson D F 1997 *Phys. Rev.* E **55** 1071
[40] Garrison J C and Chiao R Y 2004 *Phys. Rev.* A **70** 053826
[41] Feigel A 2004 *Phys. Rev. Lett.* **92** 020404
[42] Leonhardt U 2006 *Phys. Rev.* A **73** 032108
[43] Raabe C and Welsch D-G 2005 *Phys. Rev.* A **71** 013814
[44] Welsch D-G and Raabe C 2005 *Phys. Rev.* A **72** 034104
[45] Raabe C and Welsch D-G 2005 *J. Opt. B: Quantum Semiclass.* **7** 610
[46] Raabe C and Welsch D-G 2006 *Preprint* quant-ph/0602059
[47] Zhang J Z and Chang R K 1988 *Opt. Lett.* **13** 916
[48] Lai H M, Leung P T, Poon K L and Young K 1989 *J. Opt. Soc. Am.* B **6** 2430
[49] Brevik I and Kluge R 1999 *J. Opt. Soc. Am.* B **16** 976
[50] Lambrecht A, Nesvizhevsky V V, Onofrio R and Reynaud S 2005 *Class. Quantum. Grav.* **22** 5397

[51] McGuirk J M, Harber D M, Obrecht J M and Cornell E A 2004 *Phys. Rev.* A **69** 062905
[52] Schwinger J, DeRaad L L and Milton K A 1978 *Ann. Phys.* **115** 1
[53] Matloob R and Falinejad H 2001 *Phys. Rev.* A **64** 042102
[54] Ellingsen S A 2006 *Master's Thesis* Department of Physics, Norwegian University of Science and Technology
[55] Tomaš M S 2002 *Phys. Rev.* A **66** 052103
[56] Langbein D 1974 *Theory of Van der Waals Attraction (Springer Tracts in Modern Physics* vol 72*)* (Berlin: Springer)
[57] Parsegian V A 2006 *Van der Waals Forces* (Cambridge: Cambridge University Press)
[58] Scardicchio A and Jaffe R L 2004 *Nucl. Phys.* B **704** 552
[59] Chaudhury M K 1984 Short-range and long-range forces in colloidal and macroscopic systems *PhD Thesis* Faculty of the Graduate School, State University of New Yourk on Buffalo
[60] Torgerson J R and Lamoreaux S 2004 *Phys. Rev.* E **70** 047102
[61] Pirozhenko I, Lambrecht A and Svetovoy V B 2006 *New J. Phys.* **8** 238
[62] Brevik I, Aarseth J B, Høye J S and Milton K A 2004 *Proc. 6th Workshop on Quantum Field Theory under the Influence of External Conditions* ed K A Milton (Paramus, NJ: Rinton Press) p 54 (*Preprint* quant-ph/0311094)
[63] Jaekel M-T, Lambrecht A and Reynaud S 2002 *New Astron. Rev.* **46** 727
[64] Jaekel M-T and Reynaud S 1992 *J. Phys. I France* **2** 149
[65] Milonni P W and Chernobrod B M 2004 *Nature* **432** 965
[66] Karrai K 2006 *Nature* **444** 41
[67] Arcizet O, Cohadon P-F, Briant T, Pinard M and Heidmann A 2006 *Nature* **444** 71
[68] Kleckner D and Bouwmeester D 2006 *Nature* **444** 75
[69] Buenzli P R and Martin Ph A 2005 *Europhys. Lett.* **72** 42